Available at
http://pvamu.edu/aam
Appl. Appl. Math.
ISSN: 1932-9466

AAM Special Issue No. 4 (March 2019), pp. 117 - 134

Applications and Applied Mathematics:
An International Journal
(AAM)

MHD Boundary Layer Flow of Darcy-Forchheimer Mixed Convection in a Nanofluid Saturated Porous Media with Viscous Dissipation

[1]S. Jagadha and [2]P. Amrutha

[1]Department of Mathematics
Institute of Aeronautical Engineering
Hyderabad, T.S., India
jagadhasaravanan@gmail.com

[2]Department of Mathematics
St. Ann's college for women, Mehdipatnam
Hyderabad, T.S., India

Received: August 4, 2018; Accepted: October 28, 2018

Abstract

The steady laminar viscous incompressible nanofluid flow of mixed convection and mass transfer about an isothermal vertical flat plate embedded in Darcy porous medium in the presence of magnetic field and viscous dissipation is analyzed. The governing partial differential equations are converted into ordinary differential equations by similarity transformations. The coupled nonlinear ordinary differential equations are linearized by Quasi-linearization technique. The linear ordinary differential equations are solved by using implicit finite difference scheme with the help of C-programming. Numerical calculations are carried out for different values of dimensionless parameter such as magnetic field, mixed convection parameter, inertia parameter, buoyancy ratio parameter, Eckert number, Prandtl number, Brownian motion parameter and Thermophoresis parameter. The temperature and concentration profiles increase with the increase of thermophoresis parameter. It is noticed that with the increase of Brownian motion parameter the temperature profile increases whereas concentration profile decreases. On the other hand, the Local Nusselt number and the local Sherwood number also presented and analyzed.

Keywords: MHD; Darcy-Forchheimer; Viscous dissipation; Brownian motion; Thermophoresis; Porous media; FDM

MSC 2010 No.: 76W05, 76D05, 76S05

1. Introduction

The nanofluid is the amalgamation of suspensions of nano-size particles into the conventional fluids which was firstly pioneered by Choi (1995). The nanoparticles involved in this fluid are made of metals, carbides and oxides or carbon nanotubes, and conventional fluids take account of water, oil and ethylene glycol. The thermal conductivity of nanoparticles is larger than that of regular fluids, and due to this fact solid particles are used to enhance the thermal properties of base fluids. So the existence of nano solid particles in the conventional fluids heat transfer characteristics enhanced. There are several potential uses of nanofluids in heat transfer such as engine cooling, refrigerator, chiller, microelectronics, and fuel cells.

The word magneto-hydrodynamics has several industrial significance such as MHD generators, pumps, petroleum technologies and liquid metal cooling blanket for fusion reactor. Forghani et al. (2017) discussed the effect of Hartmann number on flow and heat transfer of Ag-water nanofluid with variable heat flux. Ganga et al. (2017) premeditated the impact of heat generation/absorption on MHD nanofluid boundary layer flow of a nanofluid over a vertical plate utilized Buongiorno model. Again, the influence of MHD nanofluid flow over an elongating flat plate was deliberated by Hatami et al. (2016) and Sheikholeslami et al. (2015). Recently, Salahuddin et al. (2016) examined the Carreau-Yasuda fluid flow past a flat sensor surface when magnetic field is applied. Mahmoudi et al.(2015) studied the natural convection in an open cavity with non-uniform thermal radiation. Dagonchi et al. [8] investigated the consequences of thermal radiation on MHD flow of nanofluid between parallel plates. Nandy et al. (2013) scrutinized the impact of slip on the hydromagnetics stagnation point flow and heat transfer of nanofluids past an enlarging surface. Karimipour et al. (2017) analyzed numerically the flow of different nanofluids in a microchannel. Jalilpour et al. (2014) studied the MHD flow of a nanofluid towards a stretching sheet by taking into account the surface heat flux and suction/blowing. Sheri and Thumma (2016) performed a numerical study by utilizing different nano-solid particle to discuss the heat transfer enhancement in MHD flow over a vertical plate. Pal and Mandal (2015) have presented the impact of viscous-Ohmic dissipation on hydro-magnetic boundary layer flow of nanofluid over an upright stretching/ shrinking surface in the existence of thermal radiation. Naramgari and Sulochana (2016) investigated the influence of thermal radiation and suction/injection on steady hydro-magnetic flow of suspension of nanoparticles over a porous stretching/shrinking surface by considering chemical reaction.

Recently, the combined effect of viscous-Ohmic dissipation and thermal radiation on hydro-magnetic flow of nanofluid over a stretching/shrinking sheet in the presence of slip and porous medium was studied by Ganesh et al. (2016). Hayat et al. (2016) carried out a discussion over the nanofluid flow due to Riga plate with convective boundary conditions and heat generation/absorption. The repercussions of flow and heat transfer on nanofluids flow over a parallel flat plate have been observed by Ahmadi et al. (2014). They found that Nusselt number accelerated with volume fraction of nano-solid particles. Vajravelu et al. (2011) investigated the impact of nanoparticle volume fraction of nanofluids and heat transfer characteristics in the fluid flow due to a stretching surface. The authors depicted that thickness of thermal boundary layer grows with nanoparticles volume fraction. Recently, Rashidi et al. (2016) deliberated the effect of heat and mass transfer on MHD flow of micropolar nanofluid between two-coaxial parallel plates with uniform blowing and porous medium. In the past, there are some investigations on squeezing flow of nanofluid between parallel plates done by (2013-16). Ganga et al. (2015) scrutinized the influence of viscous and Ohmic dissipation, heat generation/absorption on radiative MHD flow of nanofluid over a

vertical plate. In the earlier literatures, the combined effect of porous medium and viscous dissipation on nanofluid flow for different geometry was considered by Pandey et al. (2016). Sheikholeslami et al. (2015) inspected the influence of Brownian motion and thermophoresis on a steady flow of nanofluid between parallel plates.

Ramesh et al. (2014) explored their research on stretching sheet and they analyzed the heat transfer characteristics of a nanofluid. Many researchers have studied and given valuable contribution in the field of nanofluid flows over a permeable stretching sheet. Simulation of magnetohydrodynamic CuO–water nanofluid flow and heat transfer in the presence of Lorentz forces was discussed by Sheikholeslami et al. (2014). Ellahi et al. (2013) illustrated non-Newtonian nanofluids flow through a porous medium between two coaxial cylinders by considering variable viscosity. Ellahi (2013) presented the analytical solution to analyze the effects of MHD and temperature dependent viscosity.

The present paper deals with the effects of MHD on the nanofluid flow of mixed convection and mass transfer of a steady, two-dimensional, Darcy-Forchheimer, laminar boundary layer about an isothermal vertical flat plate embedded in a porous medium in the presence of chemical reaction, viscous dissipation with nano parameters. The governing non-linear differential equations are linearized by using the Quasi-linearization technique. The implicit finite difference scheme is used to solve the coupled linear differential equations.

2. Mathematical Description of the Problem

Consider the steady, two-dimensional, Darcy-Forchheimer model and mixed convection boundary layer over a vertical flat plate of a constant temperature T_w and concentration C_w, which is embedded in a fluid saturated porous medium of ambient temperature T_∞ and concentration C_∞, respectively. The properties of the fluid and the porous medium are assumed to be constant, isotropic and homogenous. The *x*-coordinate is measured along the surface from its leading edge and the *y*-coordinate is measured normal to it. With the Boussinesq approximation and Brownian motion of particles, the governing boundary-layer equations flow from the wall to the fluid saturated porous medium are:

$$\frac{\partial u}{\partial x} + \frac{\partial v}{\partial y} = 0, \tag{1}$$

$$\left[1 + \frac{\sigma \beta_0^2 K}{\rho \nu}\right] \frac{\partial u}{\partial y} + \frac{C_f \sqrt{K}}{\nu} \frac{\partial (u^2)}{\partial y} = \pm \frac{Kg}{\nu} \left[\beta \frac{\partial T}{\partial y} + \beta^* \frac{\partial C}{\partial y}\right], \tag{2}$$

$$u \frac{\partial T}{\partial x} + v \frac{\partial T}{\partial y} = \alpha \frac{\partial^2 T}{\partial y^2} + \frac{\nu}{c_p} \left(\frac{\partial u}{\partial x}\right)^2 + \left[D_B \frac{\partial C}{\partial y} \frac{\partial T}{\partial y} + \frac{D_T}{T_\infty} \left(\frac{\partial T}{\partial y}\right)^2\right], \tag{3}$$

$$u \frac{\partial C}{\partial x} + v \frac{\partial C}{\partial y} = D \frac{\partial^2 C}{\partial y^2} + \frac{D_T}{T_\infty} \frac{\partial^2 T}{\partial y^2}. \tag{4}$$

In the above equations *u, v* are the velocity components in the *x* and *y* directions respectively, g is the acceleration due to gravity, ν is the kinematic viscosity, β and β^* are the coefficient of volume expansion and the volumetric coefficient of expansion with concentration respectively, *K* is the Darcy permeability of the porous medium, C_f , C_p are the Forchheimer coefficient and the specific heat of the fluid at constant pressure. In addition, *T* and *C* are the temperature of the fluid inside the thermal boundary layer and the corresponding concentrations. Furthermore α and *D* are the effective thermal diffusivity and the Brownian

diffusion coefficient. In Equation (2), the plus sign corresponds to the case where the buoyancy force has a component "aiding" the forced flow and the minus sign refer to the "opposing" case.

The boundary conditions are given by

$$\begin{aligned} v = 0, \quad T = T_w, \quad C = C_w \text{ as } y = 0, \\ u = u_\infty, \quad T = T_\infty, \quad C = C_\infty \text{ as } y \to \infty. \end{aligned} \tag{5}$$

It is convenient to transform the governing equations into a dimensionless form which can be suitable for solution. This can be done by introducing the dimensionless variables for mixed convection:

$$\eta = \sqrt{Pe_x}\,\frac{y}{x}\ ,\ \psi = \alpha\sqrt{Pe_x} f(\eta),\ \theta(\eta) = \frac{(T-T_\infty)}{(T_w - T_\infty)},\ \phi(\eta) = \frac{(C-C_\infty)}{(C_w - C_\infty)}, \tag{6}$$

where ψ is the stream function that satisfies the continuity equation and η is the dimensionless similarity variable. With the change of variables, Equation (1) is identically satisfied and Equations (2)-(4) are transformed, respectively, to:

$$(1 + Ha^2) f^{"} + 2\Lambda f' f^{"} = \pm\left(\frac{\mathrm{Ra}_x}{\mathrm{Pe}_x}\right)(\theta' + N\phi'), \tag{7}$$

$$\theta^{"} + \frac{1}{2} f\theta' + PrEcf^{"2} + PrN_b\theta'\phi' + PrN_t\theta'^2 = 0, \tag{8}$$

$$\phi^{"} + Le\frac{1}{2} f\phi' + \frac{N_t}{N_b}\theta^{"} = 0. \tag{9}$$

The corresponding dimensionless boundary conditions take the form:

$$\begin{aligned} f(\eta) = 0, \theta(\eta) = 1, \phi(\eta) = 1 \text{ on } \eta = 0, \\ f'(\eta) \to 1, \theta(\eta) \to 0, \phi(\eta) \to 0 \text{ as } \eta \to \infty. \end{aligned} \tag{10}$$

Here, the primes denote differentiation with respect to η, $Pr = \nu/\alpha$ is the Prandtl number, $Le = \alpha/D$ is the Schmidt number, $N = \beta^*(C_w - C_\infty)/\beta(T_w - T_\infty)$ is the buoyancy ratio parameter, $Ra_x = (Kg\beta)(T_w - T_\infty)x/\alpha\nu$ is the Rayleigh number, $Pe_x = u_\infty x/\alpha$ is the local Peclet number, $Ec = u_\infty^2/c_f(T_w - T_\infty)$ is the Eckert number, $\Lambda = c_f\sqrt{K}\,u_\infty/\nu$ is the inertia parameter, Brownian motion parameter $Nb = \tau D_B(C_w - C_\infty)/\nu$, thermophoresis parameter $Nt = \tau D_T(T_w - T_\infty)/\nu T_\infty$ and magnetic parameter $Ha^2 = \sigma\beta_o^2 k/\rho\nu$.

3. **Numerical Solution**

Applying the Quasi-linearization technique (1965) to the non-linear Equation (7) we obtain as

$$(1 + Ha^2 + 2\wedge F') f^{"} + 2\,\lambda\,\mathrm{F}^{"} f' = \pm\left(\frac{\mathrm{Ra}_x}{\mathrm{Pe}_x}\right)(\theta' + N\phi') + 2 \wedge F^{"} F', \tag{11}$$

where assumed F is the value of f at n^{th} iteration and f' is at $(n+1)^{th}$ iteration. The convergence criterion is fixed as $|F - f| < 10^{-5}$.

Using an implicit finite difference scheme for the Equation (8), (9) and (11) we obtain

$$a[i]\, f\left[i-1\right]+b[i]\, f\,[i]+c[i]\, f\left[i+1\right]=d\,[i],$$

$$a_1[i]\theta[i-1]+b_1[i]\theta[i]+c_1[i]\theta[i+1]=d_1[i],$$

$$a_2[i]\phi[i-1]+b_2[i]\phi[i]+c_2[i]\phi[i+1]=0\,,$$

where

$$a[i]=\ 1+[Ha]^2\ +2\Lambda F_1[i]-0.5*h*2\Lambda F_2[i],$$

$$b[i]=-2*\left(1+Ha^2+2\Lambda F_1[i]\right),$$

$$c[i]=1+Ha^2+2\Lambda F_1[i]\ +0.5*h*2\Lambda F_2[i],$$

$$d[i]=h*h*\pm\left(\frac{Ra_x}{Pe_x}\right)\left(\theta_1+N\phi_1\right)+2\Lambda F_2[i]F_1[i],$$

$$a_1[i]=\ 1-0.5*h*0.5*\ f\,[i]+PrNb\phi_1+2PrNt\theta_1,$$

$$b_1[i]=-2,$$

$$c_1[i]=1+0.5*h*0.5*\ f\,[i]+PrNb\phi_1+2PrNt\theta_1,$$

$$d_1[i]=h*h*-Pr\,Ec\ f_2[i]*\ f_2[i]+\theta_1*\theta_1,$$

$$a_2[i]=1\ -0.5*h*Le*0.5*\ f\,[i],$$

$$b_2[i]=-2,$$

$$c_2[i]=1+0.5*h*Le*0.5*\ f\,[i],$$

$d_2[i]=h*hD_2[i]$, and

$$A[i]=\ 1+Ha^2+2\Lambda F_1[i],$$

$$B[i]=2\Lambda F_2[i],\ D[i]=\pm\left(\frac{Ra_x}{Pe_x}\right)\left(\theta_1+N\phi_1\right)+2\Lambda F_2[i]F_1[i],$$

$$A_1[i]=1,\ B_1[i]=0.5*\ f\,[i]+PrNb\phi_1+2PrNt\theta_1,$$

$$D_1[i] = -Pr\,Ec\,f_2[i] * f_2[i] + \theta_1 * \theta_1,$$

$$A_2[i] = 1,\ B_2[i] = Le * 0.5 * f[i],\ D_2 = -\frac{Nt}{Nb}\theta_2.$$

4. Results and Discussion

The system of nonlinear ordinary differential Equations (7)-(9) together with boundary conditions (10) are locally similar and solved numerically by using implicit finite difference scheme. The coupled nonlinear differential equations, first linearized by using the Quasi-linearization technique. The implicit finite difference scheme is applied to the coupled differential equation. The resulting algebraic system is solved by Gauss- Seidel method. To compute the numerical values we have used the C programming code. To get the physical insight of the problem, this method is adequate and gives accurate result for boundary layer equations. A uniform grid was adopted, which is concentrated towards the wall. The calculations are repeated until some convergent criterion is satisfied and the calculations are stopped $|F - f| \leq 10^{-5}$. In the present study, the boundary conditions for η at ∞ are replaced by a sufficient large value of η where the velocity approaches 1, at temperature and concentration approaches zero. In order to see the effects of step size h run the code for our model with two different step sizes as $h = 0.001$ and 0.05 and in each case we found very good agreement between them on different profiles. A parameter study of physical parameter is performed to illustrate interesting features of numerical solutions.

The results of parametric study are shown graphically in Figures 1 to 9 and discussed. In the present study we have adopted the following default parameter values for numerical computation $Pr = 0.73, \frac{Ra_x}{Pe_x} = 1,\ Nb = 0.1,\ Nt = 0.1,\ N = 2, \Lambda = 1$ and $Ha = 1$.

The effects of magnetic field parameter Ha on velocity, temperature and concentration profiles are plotted in Figures 1(a)-(c) respectively. It is clear from 1(a) that the velocity of the fluid decreases with the increase of magnetic parameter Ha, while the temperature of the fluid and concentration of the fluid increases with the increase of magnetic field parameter are shown in Figures 1(b)-(c). A magnetic strength increases the Lorentz force, which opposes the flow, also increase and leads to enhance the deceleration of the flow. This result qualitatively agrees with the expectation since the magnetic field exerts retarding force on the mixed convection flow.

Figures 2(a)-(c) present the trend of the velocity, temperature and concentration for the various values of mixed convection parameter respectively. When $\frac{Ra_x}{Pe_x} \gg 1$, the flow is dominated by natural convection, whereas when $\frac{Ra_x}{Pe_x} \ll 1$ the forced convection takes the leading role .When $\frac{Ra_x}{Pe_x} = 1$, the effect of natural and forced convection achieve equal importance and the flow is truly under mixed convection conditions. Since the buoyancy is aiding the flow, the mixed convection flow is taken positive value. For the opposing flow, the value of mixed convection flow is taken negative value. Figure 2(a) shows that the fluid velocity in the boundary layer increases with the increase of mixed convection parameter $\frac{Ra_x}{Pe_x}$ for aiding flow. The mixed convection parameter effect is on the velocity profiles is to increase velocity profiles with increasing mixed convection parameter. Figures 2(b) and 2(c)

show that temperature and concentration profiles as well as thermal and solutal boundary layer thickness decrease with the increase value of mixed convection parameter $\frac{Ra_x}{Pe_x}$. When the free stream and the buoyancy force are in opposite directions (opposing flow), the buoyancy force retards the fluid in the boundary layer.

In Figures 3(a)-(c) depicts the effects of buoyancy ratio parameter N on the fluid velocity, temperature and concentrations distributions respectively. As N increases, it can be observed from Figure 3(a) that the maximum velocity increases. From Figures 3(b) and 3(c) it is observed that the temperature and concentration profiles decrease with the increase of N. Figures 4(a)-(c) illustrates the effect of inertia parameter Λ on velocity, temperature and concentration profiles respectively. It is clear from the Figure 4(a) the velocity profile decrease with the increase of inertia parameter Λ. This decrease in the fluid velocity takes place because when the porous medium inertia affects increase, the form drag of the porous medium increases. It can be observed that reverse phenomena is noticed on the temperature and concentration distributions in the boundary layer increases owing to the increase in the value of inertia parameter Λ. It is well known that the presence of porous medium in the flow presents an obstacle to flow causing the flow to move slower and the fluid temperature and concentration to increase.

In Figures 5(a)-(c) the effect of viscous dissipation Ec on velocity, temperature and concentration are presented. As Eckert number Ec increases the velocity increases. With the effect of viscous dissipation the temperature profiles increases is observed from Figure 5(b). It is also noticed from Figure 5(c), the effect of viscous dissipation there is no significant changes on concentration profiles. The effect of thermophoresis parameter Nt is displayed in Figures 6(a) and 6(b) for temperature and concentration respectively. Temperature and concentration profiles increase with the increase of thermophoresis parameter. The effect of Brownian motion parameter Nb for temperature and concentration is displayed in Figure 7(a) and 7(b) respectively. With the increase of Brownian motion parameter Nb it is noticed that temperature profile increases whereas concentration profile decreases. The effect of Eckert number Ec is to reduce the Nusselt number whereas it increases in Sherwood number in Figures 8(a)-8(b). The viscous dissipation effect is more on Nusselt number when compare with the Sherwood number. The effect of buoyancy ratio N on the heat and mass transfer results in terms of $\frac{Nu_x}{\sqrt{Pe_x}}$ and $\frac{Sh_x}{\sqrt{Pe_x}}$ are displaced in Figures 9(a) and 9(b). The effect of buoyancy ratio parameter N is to reduce the value of Nusselt number and increases the Sherwood number

5. Conclusion

This work considered the effects of thermophoresis and Brownian motion parameters on Darcy Forchheimer mixed convection heat and mass transfer embedded in a nanofluid saturated porous medium under the influence of magnetic field parameter with viscous dissipation. The governing partial differential equations are transformed into a system of ordinary differential equations using similarity transformation. The non-linear ordinary differential equations are linearized by using Quasi-linearization technique and then solved numerically by using implicit finite difference scheme.

The following conclusions are drawn:

1. The velocity profile is decreased with the increase of magnetic parameter Ha, inertia parameter Λ and viscous dissipation Ec whereas reverse phenomena is observed in the case mixed convection $\frac{Ra_x}{Pe_x}$ and buoyancy parameter N.

2. The temperature profile increases with the increase of magnetic parameter Ha, inertia parameter Λ, viscous dissipation Ec, thermophoresis parameter Nt, Brownian motion parameter Nb while with the increase of mixed convection parameter $\frac{Ra_x}{Pe_x}$ and inertia parameter Λ the temperature profile decreases

3. The concentration profile is increased with the increase of magnetic parameter Ha, inertia parameter Λ, thermophoresis parameter Nt whereas the reverse phenomena is seen in mixed convection parameter $\frac{Ra_x}{Pe_x}$, buoyancy ratio parameter N and Brownian motion parameter Nb.

REFERENCES

Acharya, N., Das, K. and Kundu, P.K. (2016). The squeezing flow of Cuwater and Cu-kerosene nanofluids between two parallel plates, Alexandria Eng. J. Vol.55, pp. 1177-1186.

Ahmadi, A.R., Zahmatkesh A., Hatami M. and Ganji D.D. (2014). A comprehensive analysis of the flow and heat transfer for a nanofluid over an unsteady stretching flat plate, Powd. Technol, Vol.258, pp. 125-133.

Bellman, R.B., and Kalaba, R.E. (1965). Quasi-linearization and Non-Linear boundary value problem, Elsevier, Vol.21, pp. 183-194.

Choi, S.U.S.(1995). Enhancisng Thermal Conductivity of Fluids with Nanoparticles. ASME Publications-Fed, vol. 231, pp. 99-106.

Dogonchi, A.S., Divsalar, K. and Ganji D.D. (2016). Flow and heat transfer of MHD nanofluid between parallel plates in the presence of thermal radiation, Comput. Meth. Appl. Mech. Eng. Vol. 310, pp. 58–76.

Domairry, G. and Hatami, M. (2014). Squeezing Cu–water nanofluid flow analysis between parallel plates by DTM-Pade´ Method, J. Mol. Liq. Vol. 193, pp. 37–44.

Ellahi, R., Aziz S. and Zeeshan A. (2013).Non Newtonian nanofluids flow through a porous medium between two coaxial cylinders with heat transfer and variable viscosity, J. Porous Media, Vol.16, pp. 205-216.

Ellahi, R. (2013).The effects of MHD and temperature dependent viscosity on the flow of non-Newtonian nanofluid in a pipe: analytical solutions, Appl. Math. Model. Vol. 37, pp. 1451-1457.

Forghani, P.T., Karimipour, A., Afrand, M. and Mousavi, S. (2017). Different nano-particles volume fraction and Hartmann number effects on flow and heat transfer of water-silver nanofluid under the variable heat flux, Phys. E: Low-dim. Syst. Nanost. Vol.85, pp. 271-279.

Ganga, B., Ansari, S.M.Y., Ganesh, N.V. and Hakeem, A.A. (2016). MHD flow of Boungiorno model nanofluid over a vertical plate with internal heat generation/absorption, Prop.Power Res, Vol. 5, pp. 211-222.

Ganga, B., Ansari, S.M.Y., Ganesh N.V. and Hakeem A.A. (2015). MHD radiative boundary layer flow of nanofluid past a vertical plate with internal heat generation/absorption, viscous and Ohmic dissipation effects, J. Nigerian Math. Soc. Vol.34, No.2 , pp. 181-194.

Ganesh,,N.V., Hakeem, A.A. and Ganga, B. (2016). Darcy-Forchheimer flow of hydromagnetic nanofluid over a stretching/shrinking sheet in a thermally stratified porous medium with second order slip, viscous and Ohmic dissipations effects, Ain Shams Eng. Journal. Vol. 9, pp. 939-951.

Gupta, A.K. and Ray, S.S. (2015). Numerical treatment for investigation of squeezing unsteady nanofluid flow between two parallel plates, Powd. Technol. Vol. 279, pp. 282-289.

Hatami, M., Khazayinejad, M. and Jing, D. (2016),. Forced convection of Al2O3–water nanofluid flow over a porous plate under the variable magnetic field effect, Int. J. Heat Mass Transf. Vol. l02, pp. 622-630.

Hayat, T., Abbas, T., Ayub, M., Farooq, M. and Alsaedi, A. (2016). Flow of nanofluid due to convectively heated Riga plate with variable thickness, J. Mol. Liq. Vol. 222, pp. 854-862.

Jalilpour, B., Jafarmada,r S., Ganji, D.D., Shotorban, A.B. and Taghavifar, H. (2014).Heat generation/absorption on MHD stagnation flow of nanofluid towards a porous stretching sheet with prescribed surface heat flux, J. Mol. Liq. Vol. 195, pp. 194-204.

Karimipour, A., D'Orazio, A. and Shadloo, M.S. (2017).The effects of different nanoparticles of Al2O3 and Ag on the MHD nano fluid flow and heat transfer in a microchannel including slip velocity and temperature jump, Phys. E: Low-dim. Syst. Nanost. Vol. 86, pp.146-153.

Mahmoudi, A., Mejri, I., Abbassi, M.A. and Omri, A. (2015). Analysis of MHD natural convection in a nanofluid-filled open cavity with non-uniform boundary condition in the presence of uniform heat generation/absorption, Powd. Technol., Vol. 269, pp. 275-289.

Nandy, S.K. and Mahapatra, T.R. (2013). Effects of slip and heat generation/absorption on MHD stagnation flow of nanofluid past a stretching/shrinking surface with convective boundary conditions, Int. J. Heat Mass Transf. Vol.64, pp.1091-1100.

Naramgari, S. and Sulochana, C. (2016). MHD flow over a permeable stretching/shrinking sheet of a nanofluid with suction/injection, Alexandria Eng. J. Vol.55, pp.819-827.

Noor, N.F.M., Abbasbandy, S. and Hashim I. (2012). Heat and mass transfer of thermoporetic MHD flow over an inclined radiate isothermal permeable surface in the presence of heat source/ sink, Int. J. Heat Mass Transfer Vol.55, pp. 2122-2128.

Pal, D. and Mandal, G. (2015). Hydromagnetic convective–radiative boundary layer flow of nanofluids induced by a non-linear vertical stretching/shrinking sheet with viscous–Ohmic dissipation, Powd. Technol, Vol.279, pp.61-74.

Pandey, A.K. and Kumar, M. (2016). Natural convection and thermal radiation influence on nanofluid flow over a stretching cylinder in a porous medium with viscous dissipation, Alexandria Eng. J. Vol.56, pp.55-62.

Pandey, A.K. and Kumar, M. (2016). Effect of viscous dissipation and suction/injection on MHD nanofluid flow over a wedge with porous medium and slip, Alexandria Eng. J. Vol.55, pp. 3115-3123.

Rashidi, M.M., Reza, M. and Gupta, S. (2016). MHD stagnation point flow of micropolar nanofluid between parallel porous plates with uniform blowing, Powd. Technol. Vol.301, pp. 876-885.

Ramesh, G.K., Chamkha, A.J. and Gireesha, B.J. (2014). Magneto hydrodynamic flow of a non-Newtonian nanofluid over an impermeable surface with heat generation/absorption, J. Nanofluids, Vol. 3, pp. 78–84.

Rushi Kumar, B. (2013). MHD boundary layer flow on heat and mass transfer over a stretching sheet with slip effect, J. Naval Archit.Mar. Eng. Vol.10, pp.16-26.

Salahuddin, D.D., Malik, M.Y., Hussain, A., Bilal, S., Awais, M. and Khan, I. (2016), MHDsqueezed flow of Carreau-Yasuda fluid over a sensor surface, Alexandria Eng. Journal. Vol.56, pp. 27-34.

Sheikholeslami, M., Rashidi, M. and Ganji, D.D. (2015), Effect of nonuniform magnetic field on forced convection heat transfer of Fe3O4–water nanofluid, Comput. Meth. Appl. Mech. Eng. Vol. 294, pp.299–312.

Sheikholeslami, M. and Ganji, D.D. (2013). Heat transfer of Cu-water nanofluid flow between parallel plates, Powd. Technol. Vol.235, pp.873–879.

Sheikholeslami, M., Rashidi, M.M., AlSaad, D.M., Firouzi, F., Rokni, H.B. and Domairry, G. (2015). Steady nanofluid flow between parallel plates considering thermophoresis and Brownian effects, J. King Saud Univ. Sci. Vol.28, pp.380-389.

Sheikholeslami, M., Bandpy, M.G., Ellahi, R.and Zeeshan, A. (2014). Simulation of MHD CuO–water nanofluid flow and convective heat transfer considering Lorentz forces, J. Magn. Magn. Mater. Vol. 369, pp.69–80.

Sheri, S.R. and Thumma, T. (2016). Numerical study of heat transfer enhancement in MHD free convection flow over vertical plate utilizing nanofluids, Ain Shams Eng. J. Vol. 9, pp. 1169-1180.

Subhas Abel, M., Sanjayanand, E. and Nandeppanavar, M.M. (2008). Viscoelastic MHD flow and heat transfer over a stretching sheet with viscous and Ohmic dissipations, Commun. Nonlinear Sci. Numer. Simul. Vol.13, pp. 1808–1821.

Vajravelu, K., Prasad K.V., Lee J., Lee C., Pop I. and Van Gorder R.A. (2011). Convective heat transfer in the flow of viscous Ag–water and Cu–water nanofluids over a stretching surface, Int. J.Therm. Sci. Vol.50, No.5, pp. 843–851.

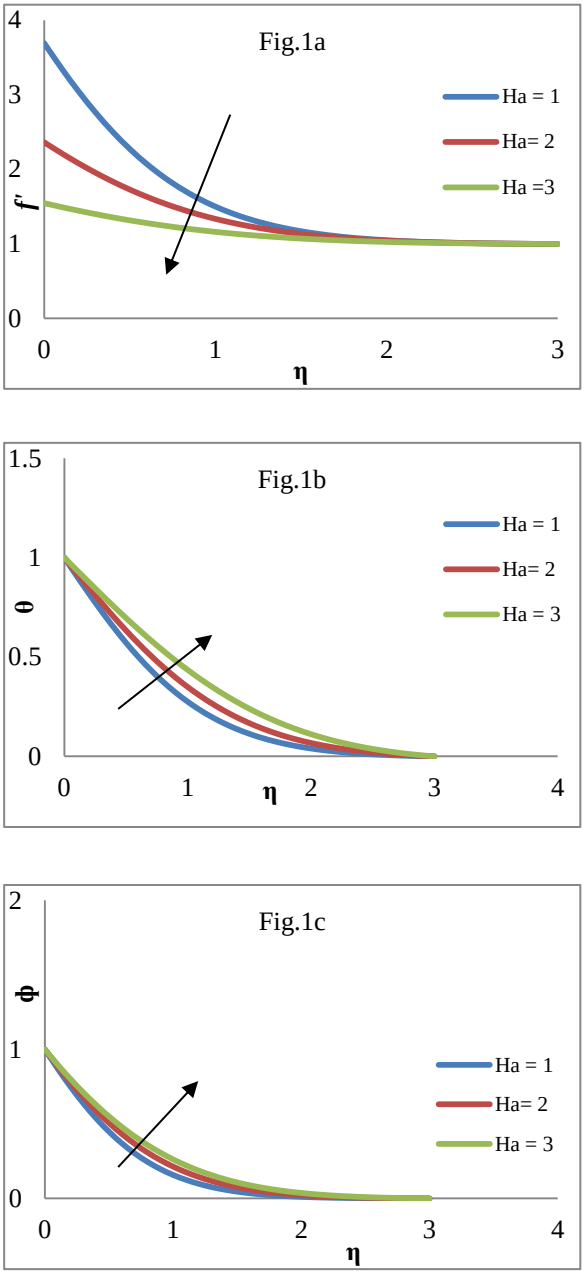

Figure 1. Effect of magnetic parameter Ha on (a) Velocity profile (b) temperature profile (c) concentration profile $\Pr = 0.73,\ \Lambda = 1,\ \frac{Ra_x}{Pe_x} = 1, N = 2, Ec = 0.5,$ $Nt = 0.1$ and $Nb = 0.1$

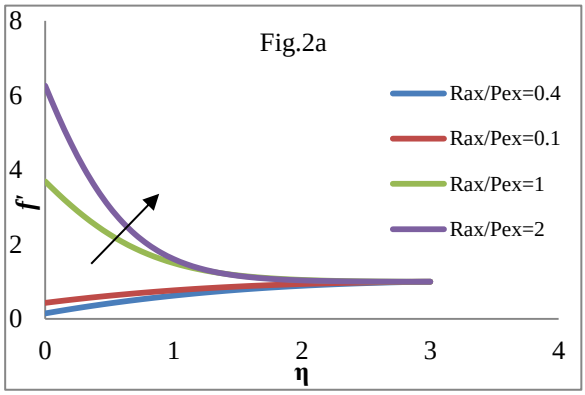

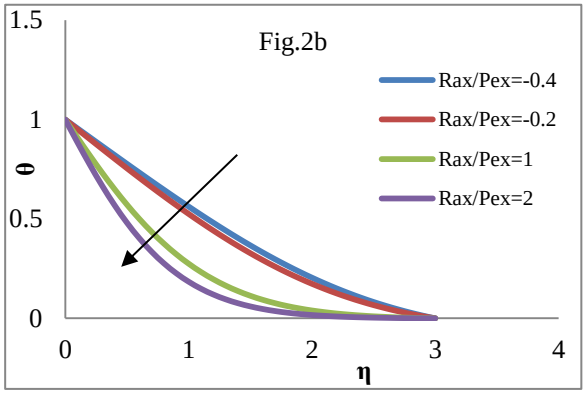

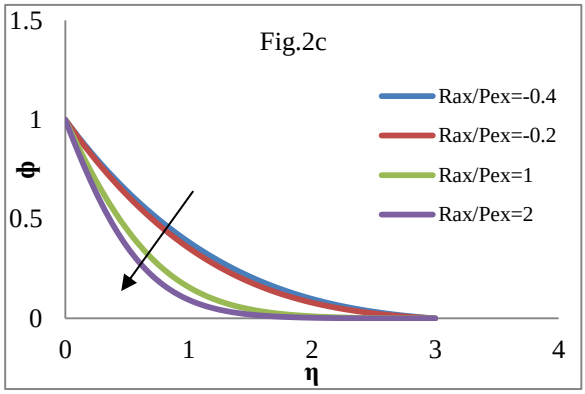

Figure 2. Effect of mixed convection parameter $\frac{Ra_x}{Pe_x}$ on (a) Velocity profile (b) temperature profile (c) concentration profile $Pr = 0.73, \Lambda = 0,\ Ha = 1, N = 2, Ec = 0.5,$ $Nt = 0.1$ and $b = 0.1$

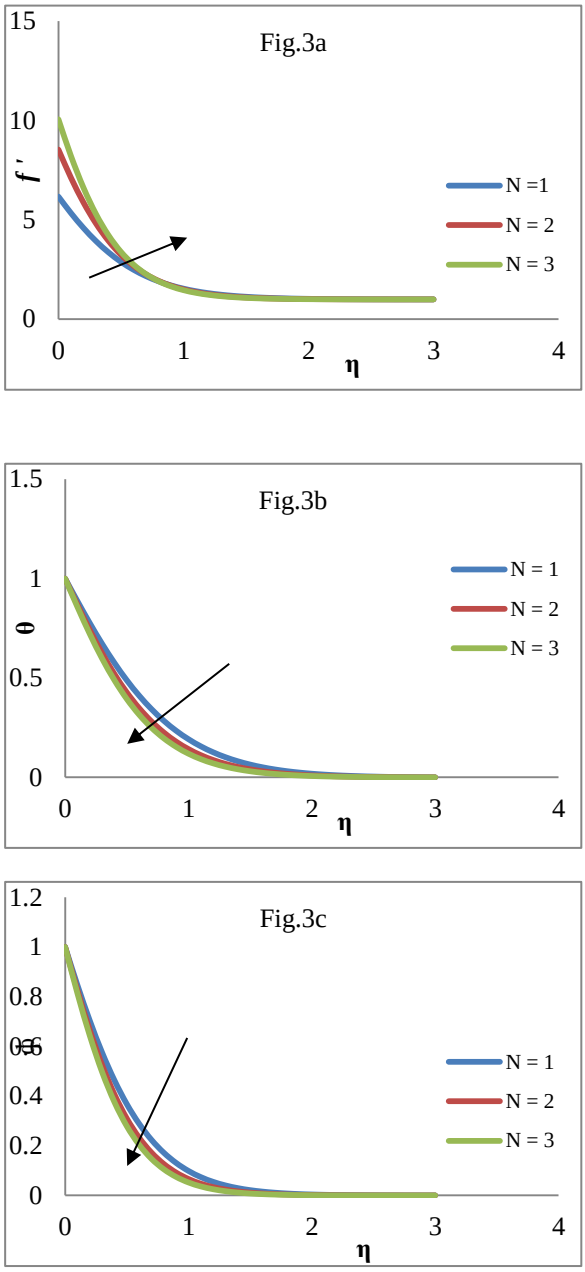

Figure 3. Effect of buoyancy ratio parameter N on (a) Velocity profile (b) temperature profile (c) concentration profile $Pr = 0.73, \Lambda = 1, Ha = 1, \frac{Ra_x}{Pe_x} = 1, Ec = 0.5, Nt = 0.1$ and $Nb = 0.1$

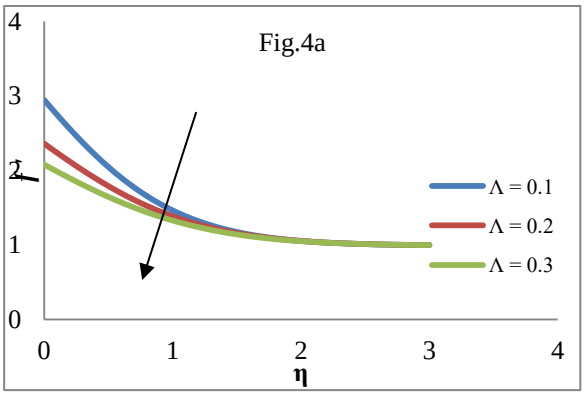

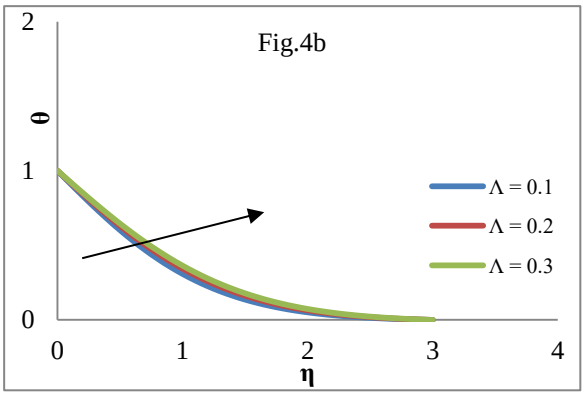

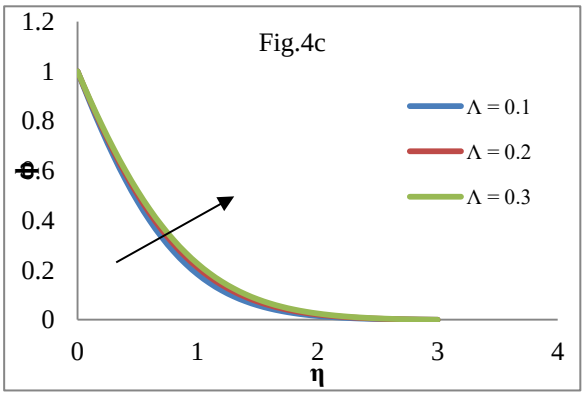

Figure 4. Effect of inertia parameter Λ on (a) Velocity profile (b) temperature profile (c) concentration profile $Pr = 0.73, N = 2,\ Ha = 1, \frac{Ra_x}{Pe_x} = 1, Ec = 0.5,$ $Nt = 0.1$ and $Nb = 0.1$

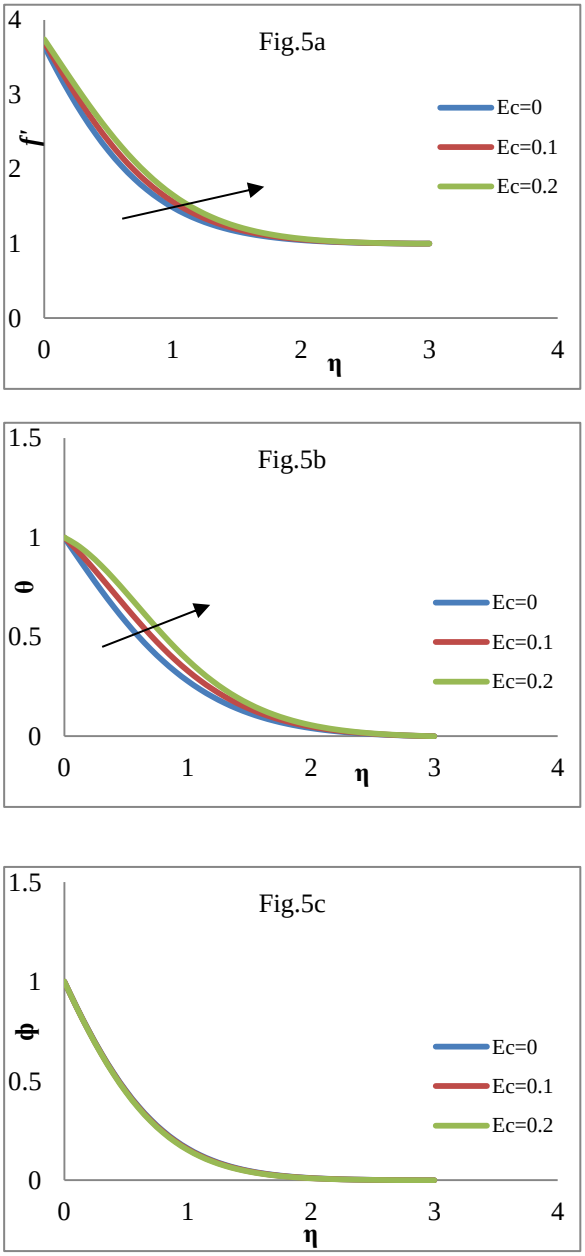

Figure 5. Effect of Eckert number Ec on (a) Velocity profile (b) temperature profile (c) concentration profile $Pr = 0.73, N = 2, Ha = 1, \frac{Ra_x}{Pe_x} = 1, \Lambda = 1,$ $Nt = 0.1$ and $Nb = 0.1$

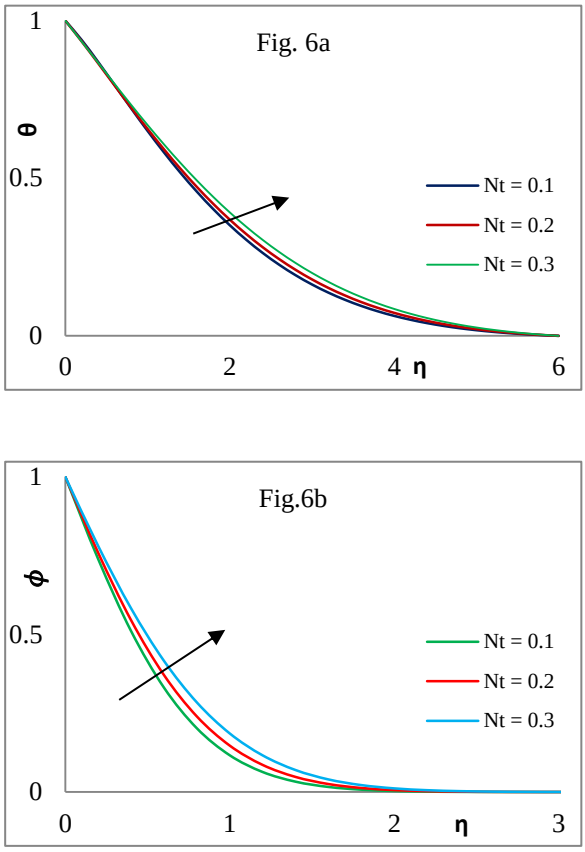

Figure 6. Effect of Thermophoresis parameter Nt on (a) temperature profile (b) concentration profile $Pr = 0.73, N = 2, Ha = 1, Ra_x/Pe_x = 1, \Lambda = 1, Ec = 0.5$ and $Nb = 0.1$

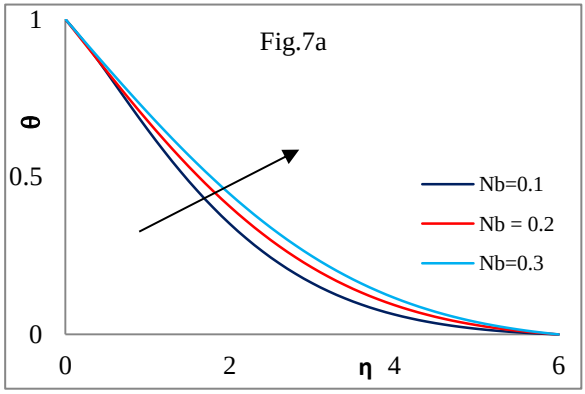

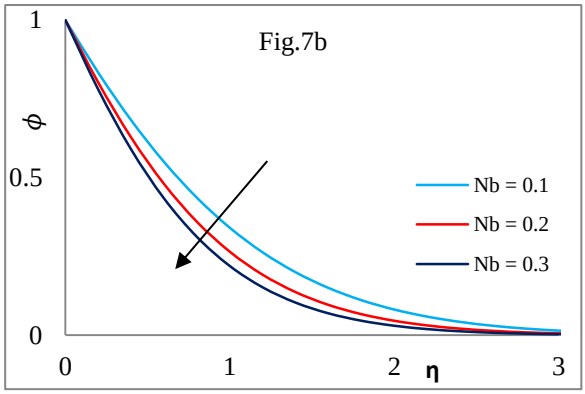

Figure 7. Effect of Brownian motion parameter on (a) temperature profile (b) concentration profile $Pr = 0.73, N = 2, Ha = 1, \frac{Ra_x}{Pe_x} = 1, \Lambda = 1, Ec = 0.5$ and $Nt = 0.1$

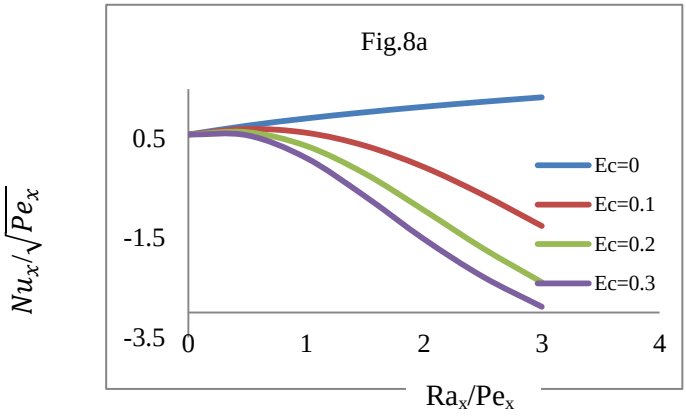

Figure 8(a). Effect of Nusselt number for various values of Eckert number, $Pr = 0.73, Ha = 1, \Lambda = 1, N = 2, Nt = 0.1$ and $Nb = 0.1$

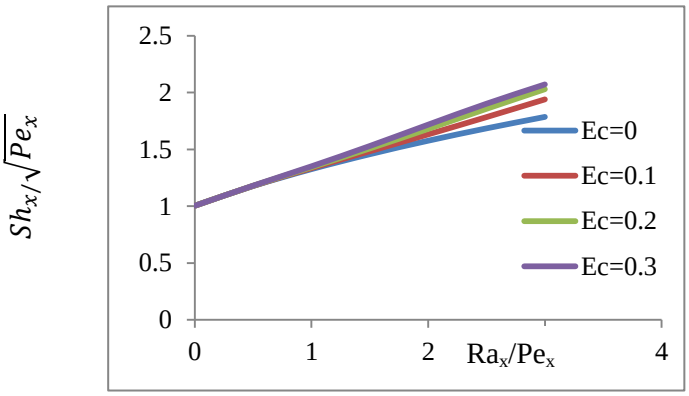

Figure 8(b). Effect of Sherwood number for various values of Eckert number, $Pr = 0.73, Ha = 1, \Lambda = 1, N = 2, Nt = 0.1$ and $Nb = 0.1$

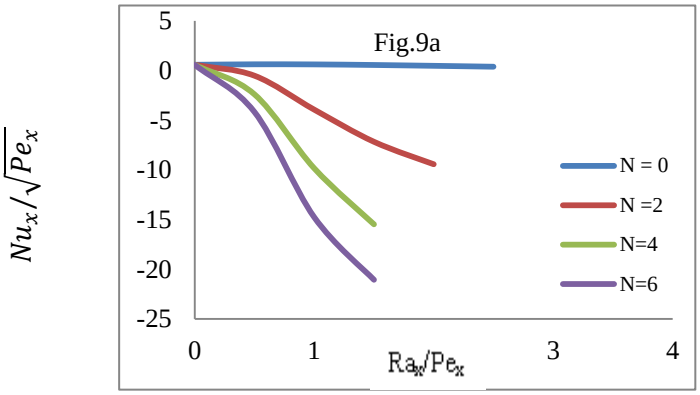

Figure 9(a). Effect of Nusselt number for various values of buoyancy ratio, $Pr = 0.73, Ha = 1, \Lambda = 1, Ec = 0.5, Nt = 0.1$ and $Nb = 0.1$

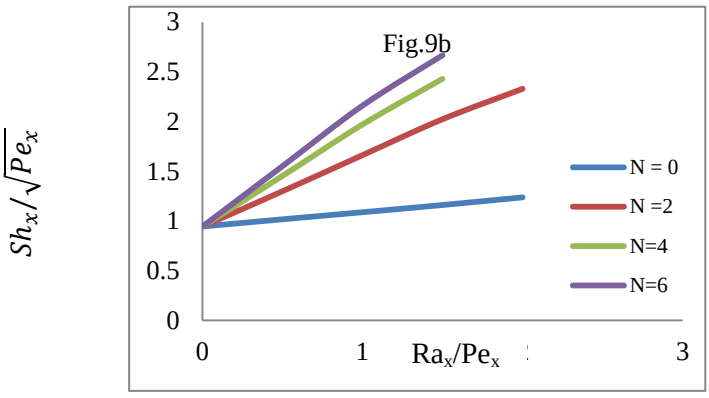

Figure 9(b). Effect of Sherwood number for various values of buoyancy ratio, $Pr = 0.73, Ha = 1, \Lambda = 1, Ec = 0.5, Nt = 0.1$ and $Nb = 0.1$